4.3 Stimulated scattering

A. Laubereau

4.3.1 Introduction

The first example of stimulated scattering was incidentally discovered in 1962 as a "new laser line in the emission of a ruby laser" [62Woo]. The phenomenon occurred when the laser was equipped with a nitrobenzene cell for Q-switching operation. The emitted frequency component was identified as an amazingly intense Raman line [62Eck] due to stimulated Raman scattering predicted theoretically in 1931 [31Goe]. Hundreds of papers appeared since then on the novel phenomenon. Compared to the wealth of experimental evidence full quantitative information about the individual scattering processes however is rather scarce since many publications confine themselves to reported frequency shifts. A quantitative analysis is also often impeded by competing nonlinear effects and by the not too well known properties of the applied laser pulses. Three cases were investigated in detail: Stimulated Raman Scattering (SRS), Stimulated Brillouin Scattering (SBS), and stimulated Rayleigh scattering.

This chapter, Chap. 4.3, follows the discussions given by Maier and Kaiser [72Mai], by Maier [76Mai], and by Penzkofer et al. [79Pen]. Circular frequencies are denoted in the following by ω_i while the corresponding frequency values are represented by $\nu_i = \omega_i/2\,\pi$. The term "circular" is often omitted in context with the ω_i's.

4.3.1.1 Spontaneous scattering processes

Fluctuations of the molecular polarizability and of the number density of atoms or molecules give rise to various scattering processes when light passes a transparent medium. The scattering is characterized by the frequency $\nu_{\rm sc}$ of the scattered light relative to the incident laser frequency $\nu_{\rm L}$, the linewidth $\delta\nu$, its polarization properties, and the scattering intensity. Here we introduce the scattering cross section $\mathrm{d}\sigma/\mathrm{d}\Omega$ relating the power $P_{\rm sc}$ of the light scattered into a solid angle $\Delta\Omega$ to the incident laser power $P_{\rm L}$:

$$P_{\rm sc} = N\,\frac{\mathrm{d}\sigma}{\mathrm{d}\Omega}\,\ell\,P_{\rm L}\,\Delta\Omega \tag{4.3.1}$$

with number density N of the (quasi-)particles generating the scattering. The interaction length is denoted by ℓ. $\mathrm{d}\sigma/\mathrm{d}\Omega$ is the differential cross section with respect to solid angle but integrated over the spectral lineshape. The spectrum of four scattering processes is depicted schematically in Fig. 4.3.1a. Two unshifted components are indicated: the narrow Rayleigh line scattered from non-propagating entropy (temperature) fluctuations and the broader Rayleigh-wing line due to orientation fluctuations of anisotropic molecules. The lines are accompanied by the Brillouin doublet representing scattering from propagating isentropic density fluctuations. In the quantum-mechanical approach the Brillouin lines are related to the annihilation (frequency up-shifted anti-Stokes component) and creation (down-shifted Stokes line) of acoustic phonons with conservation of quantum energy and (pseudo-)momentum:

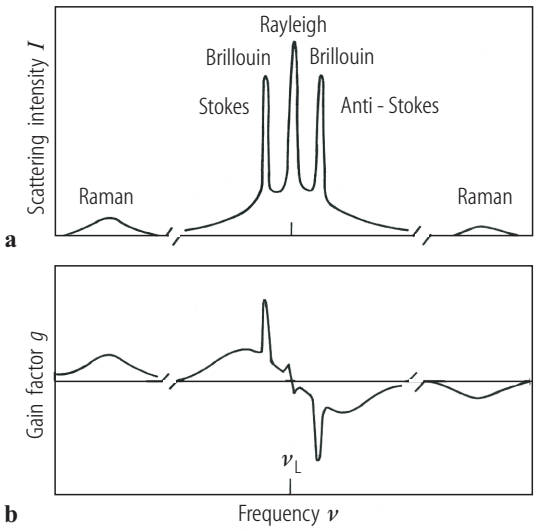

Fig. 4.3.1. (a) Schematic of the spectral intensity distribution of spontaneous light scattering in condensed matter with unshifted Rayleigh and Rayleigh-wing lines (quasi-elastic scattering) as well as Stokes- and anti-Stokes-shifted Brillouin and Raman lines (inelastic light scattering). **(b)** Frequency dependence of the corresponding gain factors of stimulated scattering (see text).

$$h\,\nu_{\mathrm{L}} = h\,\nu_{\mathrm{sc}} \pm h\,\nu_{\mathrm{o}}\ , \tag{4.3.2}$$

$$\hbar\,\boldsymbol{k}_{\mathrm{L}} = \hbar\,\boldsymbol{k}_{\mathrm{sc}} \pm \hbar\,\boldsymbol{k}_{\mathrm{o}} \tag{4.3.3}$$

with Planck's constant h and wavevector $\boldsymbol{k}$, $\hbar = h/2\,\pi$. Subscript "o" refers to the material excitation, i.e. acoustic phonons. The positive sign in (4.3.2) and (4.3.3) corresponds to the Stokes process (sc = S), while the negative sign applies for anti-Stokes scattering (sc = A). Due to the dispersion relation of acoustic phonons (phase velocity v of sound waves) the frequency shift is given by

$$\nu_{\mathrm{o}} = \frac{v k_{\mathrm{o}}}{2\,\pi} = 2\,v\,\frac{\nu_{\mathrm{L}} n}{c}\,\sin\left(\frac{\theta}{2}\right)\ . \tag{4.3.4}$$

Here c/n denotes the speed of light in the medium; θ is the scattering angle between wave vectors $\boldsymbol{k}_{\mathrm{L}}$ and $\boldsymbol{k}_{\mathrm{sc}}$ ($k_{\mathrm{sc}} \cong k_{\mathrm{L}}$, since $\nu_{\mathrm{o}} \ll \nu_{\mathrm{L}}$). Equation (4.3.4) refers to isotropic media, e.g. gases and liquids. For anisotropic solids three Brillouin doublets occur in the general case and (4.3.4) has to be modified according to the considered transverse or longitudinal acoustic phonon branch and the respective orientation-dependent sound velocity in the crystal. As a consequence of (4.3.3), $k_{\mathrm{o}} \leq 2\,k_{\mathrm{L}}$, so that only acoustic phonons close to the center of the first Brillouin zone are involved (note $k_{\mathrm{L}} \sim 10^5\ \mathrm{cm}^{-1}$).

Figure 4.3.1a also schematically shows the Stokes and anti-Stokes line of Raman scattering off a molecular vibration or off an optical phonon branch, displaying a larger frequency shift. As before, only phonons of relatively small k_{o} are involved. Polyatomic molecules display a variety of such vibrational Raman lines. In gases many vibration-rotation Raman lines occur in addition and also rotational lines with small frequency shifts. In ionic crystals the relevant material excitation is of mixed phonon-photon character and termed polariton. Since the excited states of molecular vibrations and optical phonons are weakly populated, the anti-Stokes line intensity is also small compared to the corresponding Stokes line.

A further unshifted scattering component in liquids, the Mountain line [76Ber], is only mentioned here since it was not yet observed in stimulated scattering because of its weakness and broad width. Typical values for the frequency shift ν_{o}/c and the linewidth $\delta\nu/c$ (FWHM) in wavenumber units of the various processes are given in Tables 4.3.1–4.3.5. Some scattering cross sections for the Raman interaction are listed in Table 4.3.2. The scattered light intensity is small. Even for the large

number density of condensed matter of $\sim 10^{22}$ cm^{-3} a small fraction $< 10^{-5}$ of the incident light is distributed into the whole solid angle $4\,\pi$ per cm interaction length by spontaneous scattering.

4.3.1.2 Relationship between stimulated Stokes scattering and spontaneous scattering

The elementary interaction for Stokes scattering is illustrated in Fig. 4.3.2a (solid arrows). The process involves a transition from an initial to a final energy level of the medium (horizontal lines). The relationship between the stimulated and the spontaneous process is close and originates from the Boson character of photons, i.e. the analogy of the eigenmodes of the electromagnetic field with the harmonic oscillator, the transition probability of which increases with occupation number. As a result the rate of photons scattered into an eigenmode of the Stokes field (subscript "S") depends on the occupation number n_S of this mode. Under steady-state conditions we have:

$$\frac{\mathrm{d}\,n_\mathrm{S}}{\mathrm{d}\,t} = \text{const.}\; n_\mathrm{L}\,(1 + n_\mathrm{S})\;. \tag{4.3.5}$$

The first term in the bracket on the right-hand side of (4.3.5) represents spontaneous scattering depending linearly on incident photon number n_L or laser power, compare (4.3.1), as long as $n_\mathrm{S} \ll 1$, i.e. a negligible number of scattered photons per mode of the radiation field is present. The second term on the right-hand side of (4.3.5) describes stimulated scattering that dominates for $n_\mathrm{S} > 1$ and requires sufficiently high laser intensities. In this regime an avalanche build-up of scattered photons can occur.

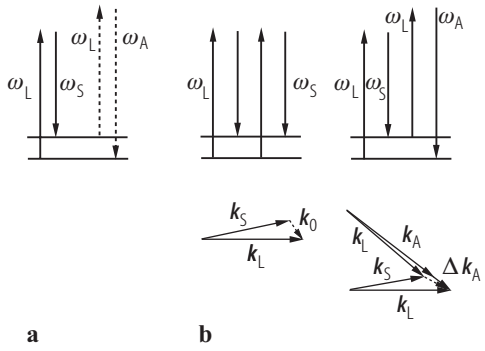

Fig. 4.3.2. (a) Schematic of the elementary scattering process of spontaneous scattering involving two energy levels (horizontal bars) of the medium with transition frequency ω_o; the Stokes (full arrows) and anti-Stokes (dashed arrows) processes are indicated. Corresponding diagrams for **(b)** stimulated Stokes scattering and **(c)** stimulated Stokes–anti-Stokes coupling in the stimulated scattering. Vertical arrows represent photons that are annihilated (upwards) or generated (downwards) in the interaction. The $\boldsymbol{k}$-vector geometries of the stimulated processes are depicted in the lower part of the figure (see text).

4.3.2 General properties of stimulated scattering

4.3.2.1 Exponential gain by stimulated Stokes scattering

Integration of (4.3.5) yields exponential growth of Stokes-scattered photons, $n_\mathrm{S} \propto \exp\,(\text{const.}\; n_\mathrm{L}\,t)$, or equivalently for forward scattering in the z-direction:

$$I_S(z) = I_S(0)\,\exp(g\,I_L\,z)\,. \tag{4.3.6}$$

Here we have replaced in the argument of the exponential the product "const. $n_L\,t$" by a more familiar term with laser intensity I_L, the gain factor g for stimulated Stokes scattering, and the interaction length z. Equation (4.3.6) indicates exponential amplification of an initial signal $I_S(0)$ that may be supplied by spontaneous scattering or by an additional input beam. The exponential growth of the scattered light is only limited by the energy conservation of (4.3.2), since for every scattered photon one incident laser photon has to be annihilated. The corresponding laser depletion leads to gain saturation not included in (4.3.6). Conversion efficiencies above 50 % have been observed for stimulated scattering in a number of cases. Equation (4.3.6) refers to steady state.

The gain factor g is an important material parameter for stimulated scattering. The dependence of g on the frequency shift of the scattering is indicated in Fig. 4.3.1b. Maximum gain occurs in the center of the down-shifted Brillouin and Raman lines (Stokes process). For stimulated Rayleigh scattering the peak gain occurs for a Stokes shift equal to half of the full width, $\delta\nu/2$, of the respective line. The negative gain values in Fig. 4.3.1b indicate loss via stimulated scattering on the anti-Stokes side.

Typical values of the peak gain factors are listed in Tables 4.3.2–4.3.5. Under steady-state conditions stimulated Brillouin scattering often represents the dominant interaction. In absorbing media additional mechanisms occur. The corresponding processes, stimulated thermal Brillouin and stimulated thermal Rayleigh scattering, are discussed below.

4.3.2.2 Experimental observation

Stimulated scattering was studied using the following three different experimental approaches:

1. generator setup,
2. oscillator setup,
3. stimulated amplification setup.

4.3.2.2.1 Generator setup

Here only an intense laser beam is directed into the sample. The kind of stimulated scattering is selected by the material and laser beam properties. As a general rule, a large gain of $g\,I_L\,z \cong 30$ is required under steady-state conditions for the traveling-wave situation with a single pass through the medium (length z), in order to observe the respective stimulated process. The scattering occurs in forward and/or backward direction because of a simple geometrical argument (maximum interaction length in these directions). The process builds up from an equivalent noise input $I_S(0)$, see (4.3.6), that can be estimated from zero point fluctuations of the electromagnetic field [79Pen]. The growth of the Stokes component is finally limited by the simultaneous decrease of incident laser radiation. The observations are difficult to analyze because of the competition of nonlinear interactions including optical self-focusing. The latter is often involved in liquid media. The observed frequency shift of the stimulated process may slightly deviate from the value known from spontaneous scattering (up to a few cm^{-1} in SRS) because of simultaneous self-phase modulation in the medium.

4.3.2.2.2 Oscillator setup

An optical resonator made up by mirrors or reflecting surfaces can provide feedback of the stimulated Stokes radiation so that the effective interaction length is increased by multiple passes

through the medium. As a result the laser intensity requirements are lowered. The scattering angle is controlled by the cavity axis, so that off-axis emission is possible relative to the laser beam. The frequency-dependent feedback and the lower intensity level of the setup can be sufficient to select a specific stimulated scattering process. Among different Raman transitions only the one with largest gain factor g shows up in SRS in general.

4.3.2.2.3 Stimulated amplification setup

Two well defined beams representing the laser component and the incident Stokes radiation are directed into the scattering medium. Scattering angle and mechanism are determined by the direction and frequency shift of the incident Stokes beam. A second tunable laser is used for the latter in general. The pump intensity I_L is smaller by one or more orders of magnitude compared to the generator case, so that self-focusing and other competing effects including secondary scattering processes can be avoided. Quantitative information on the amplitude and/or frequency dependence of the gain factor $g(\nu_\mathrm{S})$ may be deduced from careful measurements of the amplification factor.

An example for the technique is Raman gain spectroscopy that is often applied in the low-intensity limit $g\, I_\mathrm{L}\, z \ll 1$. An alternative is Raman loss spectroscopy of the transmitted laser component, since the production of Stokes photons corresponds to the annihilation of the same number of laser photons.

4.3.2.3 Four-wave interactions

4.3.2.3.1 Third-order nonlinear susceptibility

Stimulated Stokes scattering can be treated as a four-photon (or four-wave) interaction involving the third-order nonlinear susceptibility $\chi^{(3)}(-\omega_\mathrm{S}; \omega_\mathrm{L}, -\omega_\mathrm{L}, \omega_\mathrm{S})$. The interaction is illustrated by the energy level scheme of Fig. 4.3.2b. The two waves are resonantly coupled via a difference frequency resonance, $\omega_\mathrm{L} - \omega_\mathrm{S} = \omega_\mathrm{o}$, to the relevant material excitation. The latter is enhanced by the scattering thus increasing the coupling strength. The photons at frequencies ω_L and ω_S enter the process twice (see Fig. 4.3.2a). Stimulated amplification is provided in the resonant case by the imaginary part χ_3'' of $\chi^{(3)}$, while the real part leads to frequency modulation. The gain factor is related to the imaginary part by:

$$g \propto |\chi_3''|^2 \,. \tag{4.3.7}$$

Outside difference frequency resonances the real part of $\chi^{(3)}$ is also important for stimulated amplification. The general case of stimulated 4-photon amplification is treated in [79Pen]. The (fourth-rank) tensor character of $\chi^{(3)}$ is omitted here for brevity considering only parallel polarization of the light field components.

The corresponding wave-vector diagram is shown in the lower part of Fig. 4.3.2b. The general case with off-axis geometry is considered. The scattering couples to a material excitation with wave vector $\boldsymbol{k}_\mathrm{o}$. The effective scattering angle is strongly influenced by interaction-length arguments. Because of the maximum interaction length, geometries with approximate forward and backward scattering are most important. In cases where the corresponding frequency shift ω_o vanishes, e.g. SBS, stimulated scattering exactly in forward direction is not possible. For backward scattering of short pulses, e.g. SRS of a picosecond laser, the interaction length ℓ may be governed by the duration t_p (FWHM of intensity envelope) of the incident laser pulse setting an upper limit of $\ell = t_\mathrm{p}/2\, v_\mathrm{g}$ (v_g: group velocity). In forward direction a less stringent limitation is set by group velocity dispersion between laser and Stokes pulses, $\ell = t_\mathrm{p}\, \Delta(1/v_\mathrm{g})$. As a result SRS of picosecond pulses preferentially occurs in forward direction.

4.3.2.3.2 Stokes–anti-Stokes coupling

The stimulated Stokes scattering can be impeded by simultaneous anti-Stokes scattering, $\omega_A = \omega_L + \omega_o$. The anti-Stokes process is depicted in Fig. 4.3.2a (dashed arrows) and "consumes" material excitation, so that (4.3.6) is not applicable. The corresponding four-wave interaction via $\chi^{(3)}(-\omega_A; \omega_L, \omega_L, -\omega_S)$ is termed Stokes–anti-Stokes coupling and depicted in Fig. 4.3.2c. The significance of the process is determined by its wave vector mismatch Δk_A , depicted in the lower part of Fig. 4.3.2c, and the initial intensity ratio $I_A(0)/I_S(0)$ (I_A : anti-Stokes intensity). Δk_A is governed by the scattering angle and the color dispersion of the refractive index $n(\omega)$ of the medium since

$$k_i = n(\omega_i)\,\frac{\omega_i}{c}\;; \quad (i = \mathrm{A, L, S})\;. \tag{4.3.8}$$

For a collinear geometry we simply have $\Delta k_A = k_A + k_S - 2k_L$. For $\Delta k_A = 0$ and $I_A/I_S = 1$, the inverse process of anti-Stokes scattering fully inhibits stimulated Stokes scattering. An example in this context is exact forward scattering in gases, where Δk_A is small, so that the observed weakness of SRS in exact forward direction is explained in this way. For a large mismatch, $|\Delta k_A| > 3\,g\,I_L$, on the other hand, the Stokes–anti-Stokes coupling is negligible. This condition is always fulfilled for backward scattering so that simultaneous anti-Stokes scattering cannot perturb the stimulated Stokes process notably. For $I_A \ll I_S$, the perturbation of Stokes scattering by anti-Stokes production is negligible, too. In this case the process of Fig. 4.3.2c is also called Coherent Anti-Stokes Raman Scattering, CARS, an important nonlinear spectroscopy (preferentially applied for phase-matching geometries, $\Delta k_A \cong 0$).

Outside Raman resonances the properties of Stokes–anti-Stokes coupling differ notably from the near-resonant case considered here.

4.3.2.3.3 Higher-order Stokes and anti-Stokes emission

For high conversion efficiency of the stimulated scattering the Stokes intensity I_S becomes comparable to the incident radiation I_L , and the material excitation is significant. As a consequence secondary processes show up, generating a cascade of higher-order Stokes and anti-Stokes lines with relative frequency shift ω_o and decreasing intensity levels. Two mechanisms are relevant here:

1. stimulated Stokes scattering where the intense first-order Stokes component serves as the pump radiation for generating the second-order line and so forth;
2. coherent Stokes or anti-Stokes scattering off the material excitation generated by the primary Stokes scattering producing new frequency-shifted lines. The mechanism is effected by wavevector mismatches of the individual processes.

The Stokes–anti-Stokes coupling discussed above is responsible for the generation of the first-order anti-Stokes component. Higher-order Stokes scattering limits the energy conversion efficiency of first-order Stokes production. The higher-order stimulated scattering should be distinguished from higher-order spontaneous scattering since only a fundamental material transition is involved in the former case.

4.3.2.4 Transient stimulated scattering

The build-up of a material excitation in stimulated scattering involves the response time T_2 (dephasing time) of the medium. When the pulse duration t_p of the incident laser is comparable to or smaller than T_2 , the interaction becomes less efficient and the actual gain of the stimulated Stokes

process is smaller than in the steady state. Equation (4.3.6) for the stationary case is not valid for $t_p/T_2 < 10$. The smaller transient gain for a given input situation may be overcome experimentally by increased pump intensities. For details the reader is referred to the literature [78Lau]. Here only three remarks are given:

1. For homogeneous broadening of the material transition ω_o involved in the stimulated scattering the relaxation time can be simply derived from the linewidth $\delta\nu$ (FWHM)

$$T_2 = (\pi\,\delta\nu)^{-1} = \frac{1}{\Gamma}\,. \tag{4.3.9}$$

   For inhomogeneous broadening (4.3.9) may be also used to estimate an effective T_2^* from the line broadening that may be sufficient for a semi-quantitative discussion of the transient scattering. For the competition among different Raman transitions in transient SRS both gain factor g and dephasing time T_2 are relevant.
2. For frequency-modulated laser pulses the temporal behavior is not fully described by the duration t_p of the pulse envelope. Because of intensity fluctuations the effective duration of the pulse can be estimated to be $t_p^* \cong (2\,\delta\nu_L)^{-1} < t_p$ ($\delta\nu_L$: frequency width (FWHM) of the laser pulse). To ascertain steady-state conditions the condition

$$\frac{t_p^*}{T_2} > 10 \tag{4.3.10}$$

   should be fulfilled.
3. Choice of a short t_p may allow to suppress stimulated scattering of transitions with longer T_2 that would have to occur in a less favorable transient situation. An example is SRS in liquids in forward direction with picosecond pulses that is observed in spite of the larger stationary gain factor of SBS. Here the different interaction lengths of forward (SRS) and backward scattering (SBS) also play a role.

4.3.3 Individual scattering processes

4.3.3.1 Stimulated Raman scattering (SRS)

The gain constant for stimulated amplification of the first Stokes component (4.3.6) at resonance, $\omega_S = \omega_L - \omega_o$ is given by

$$g_S = \frac{4\,\pi^2\,N\,(\partial\alpha/\partial q)^2\,\omega_S}{n_L\,n_S\,c^2\,m\,\omega_o\,\Gamma}\,. \tag{4.3.11}$$

Here N denotes the molecular number density. A highly polarized vibrational Raman line with halfwidth Γ (HWHM, isotropic scattering component) is considered. $(\partial\alpha/\partial q)$ is the isotropic part of the Raman polarizability (derivative of the molecular polarizability with respect to the vibrational coordinate q of transition ω_o). m represents the reduced mass of the molecular vibration. n_i ($i = $ L, S) is the refractive index at frequency ω_i. $(\partial\alpha/\partial q)$ is connected to the Raman scattering cross section by the relation:

$$\frac{\mathrm{d}\sigma}{\mathrm{d}\Omega} = \frac{(\partial\alpha/\partial q)^2\,\omega_S^4\,h\,n_S}{4\,\pi\,c^4\,m\,\omega_o\,n_L}\,. \tag{4.3.12}$$

The frequency dependence of the gain factor is given by:

$$g(\omega_S) = \frac{g_S \, \Gamma^2}{(\omega_S - \omega_L + \omega_o)^2 + \Gamma^2} \; . \tag{4.3.13}$$

A Lorentzian lineshape is assumed in (4.3.13) that holds well in gases at sufficiently high pressure, weakly associated liquids and solids. SRS of notably depolarized Raman lines is discussed in [78Lau]. Frequency shifts observed for SRS in the generator setup are compiled in Table 4.3.1. A list of gain factors g_S and other parameters is presented in Table 4.3.2. The relaxation time T_2 in condensed matter is in the range 10^{-12} to 10^{-10} s.

Table 4.3.1. Frequency shifts (in wavenumber units) observed in stimulated Raman scattering of various materials.

(a) Liquids

Medium	Stokes shift ν_0/c [cm^{-1}]	Excitation wavelength [nm]	Reference
Acetic acid	2944		[84Kru]
Acetone	2925	527	[68Bre, 69Col]
Aniline	997	694	[66Eck]
Benzaldehyde	1001	694	[66Bar]
Benzene	992	527	[67Sha, 68Bre, 69Col, 70Alf]
Benzene	3064	694	[66Eck]
Benzene-d_6	944	694	[67Blo]
Benzonitrile	2229	694	[66Eck]
Bromobenzene	998, 1000	527, 694	[66Eck, 67Sha]
Bromopropane	2962	694	[66Bar]
2-Bromopropane	2920	694	[66Bar]
1-Bromopropane	2935	694	[66Bar]
Butyl-benzene (tert.)	1000	694	[66Bar]
Carbondisulfide	656	527	[67Sha, 68Bre, 69Col, 70Alf]
Carbontetrachloride	460	694	[66Eck]
Chlorobenzene	1002	527	[67Sha, 69Col]
Chloromethylbutane	2927	694	[66Bar]
Chloroform	663	694	[66Eck]
Cyclohexane	2825		[84Kru]
Cyclohexanone	2683	694	[66Eck]
1,3-Dibromobenzene	992	694	[66Bar]
1,2-Dichloroethane	2958		[84Kru]
Dichloromethane	2989		[75Lau]
2,2-Dichlorodiethylether	2938	527	[83Tel]
1,2-Diethylbenzene	2934	694	[66Bar]
1,2-Dimethylcyclohexane	2853, 2921	694	[66Bar]
1,4-Dimethylcyclohexane	2876	694	[66Bar]
Dimethylhexadiene	2910	694	[66Bar]
1,4-Dioxane	2967		[84Kru]
DMSO, dimethylsulfoxide	2911		[95Go]
Ethanol	2928	527	[69Col, 71Lin]
Ethyl-Benzene	1002	694	[66Eck]
1-Fluoro-2-chlorobenzene	1034	694	[66Bar]
Fluorobenzene	1009	694	[66Eck]
Fluoromethane	2970	694	[78Map]
Isopropanol	2882	527	[69Col]
Methanol	2835	527	[69Col, 70Alf]
Methanol-d_4	2200	527	[73Lau]
3-Methylbutadiene	1638	694	[66Eck]

(continued)

Table 4.3.1a continued.

Medium	Stokes shift ν_0/c [cm^{-1}]	Excitation wavelength [nm]	Reference
Nitrobenzene	1344	527, 694	[67Blo, 67Sha, 69Col]
2-Nitropropane	2945	694	[66Bar]
Nitrogen ($T = 77$ K)	2326	527	[74Lau]
1,3-Pentadiene	1655	694	[66Eck]
Piperidine	2933	694	[66Eck]
Pyridine	992	694	[66Eck]
Siliciumtetrachloride	425	527	[71Lau]
Styrene	1315, 1631, 3056	694	[66Eck]
Tintetrabromide	221	527	[78Lau]
Tintetrachloride	368	527	[78Lau]
Tetrachloroethane	2984	694	[66Eck]
Tetrachloroethylene	448, 2939	527	[69Col, 72Lau, 66Bar]
Tetrahydrofuran	2849	694	[66Eck]
Toluene	1004	527, 694	[67Blo, 67Sha]
Water	3450	527	[68Bre, 69Col, 69Rah]
m-Xylene	2933	694	[66Eck]
o-Xylene	2913	694	[66Eck]
p-Xylene	2998	694	[66Eck]

(b) Solids

Medium	Stokes shift ν_0/c [cm^{-1}]	Excitation wavelength [nm]	Reference
Al_2O_3	416	532	[97Kam2]
1-Bromonaphthalene	1363	694	[66Eck]
Calcite	1086	527	[69Col]
1-Chloronaphthalene	1368	694	[66Eck]
Diamond	1332	527	[71Lau]
2-Ethylnaphthalene	1382	694	[66Bar]
$Gd_2(MoO_4)_3$	960	532	[97Kam1]
$LiHCOO \cdot H_20$	104, 1372	694	[90Lai]
$NaClO_3$	936	532	[97Kam3]
Naphthalene	1380	694	[66Eck]
Polydiacetylene	1200		[94Yos]
Sulfur	216, 470	694	[66Eck]

(c) Gases

Medium	Stokes shift ν_0/c [cm^{-1}]	Excitation wavelength [nm]	Reference
Ammonia	3339		[72Car]
Barium vapor	11395	552	[83Sap, 87Glo]
Ethylene (55 atm)	1344	694	[70Mac]
Butane (90 atm)	2920	694	[70Mac]
Carbondioxide (20–50 atm)	1385	694	[70Mac, 78Map]
Carbonmonoxide	2145	694	[72Car]

(continued)

Table 4.3.1c continued.

Medium	Stokes shift ν_0/c [cm^{-1}]	Excitation wavelength [nm]	Reference
Cesium vapor	14597		[84Har]
Chlorine	556	694	[72Car, 78Map]
Deuterium	2991	694	[67Blo]
Hydrogen	4160	694	[67Blo, 75Cha]
Hydrogenbromide (20 atm)	2558	694	[70Mac, 78Map]
Hydrogenchloride (35 atm)	2883	694	[70Mac, 78Map]
Methane (10 atm)	2917		[70Mac]
Nitrogen (55–100 atm)	2330	694	[70Mac, 75Cha]
N_2O (50 atm)	774	694	[70Mac, 78Map]
NO	1877	694	[72Car]
Oxygen (50–100 atm)	1550	694	[70Mac]
SF_6 (15–20 atm)	1551	694	[70Mac]
SF_6 (18 atm)	775	694	[72Car]

Table 4.3.2. Gain factor and other parameters of stimulated Raman scattering.

(a) Liquids

Medium	Stokes shift ν_0/c [cm^{-1}]	Scattering coefficient $N \times d\sigma/d\Omega$ [10^7 m^{-1} sr^{-1}]	Linewidth $\delta\nu/c$ [cm^{-1}]	Gain factor g_S [10^{12} m/W]	Excitation wavelength [nm]	Ref.
Acetone	2925		17.4	12	530	[69Col]
Benzene	992		2.2	28	694	[72Mai]
Bromobenzene	1000	15	1.9	15	694	[72Mai]
Carbondisulfide	655	75	0.50	240	694	[72Mai]
Chlorobenzene	1002	15	1.6	19	694	[72Mai]
Ethanol	2928		17.4	51	530	[69Col]
Isopropanol	2882		26.7	9.2	530	[69Col]
Methanol	2834		18.7	23	530	[69Col]
Methanol	2944		26.5	18	530	[69Col]
Nitrogen	2326	2.9	0.067	170	694	[72Mai]
Nitrobenzene	1345	64	6.6	21	694	[72Mai]
Oxygen	1552	4.8	0.117	140	694	[72Mai]
Tetrachloroethylene	447			17	598	[76Mai]
Toluene	1003	11	1.9	12	694	[72Mai]
1,1,1-Trichloroethane	2939		5.2	51	530	[69Col]
Water	3450	430		1.4	530	[69Col]

(b) Solids

Medium	Stokes shift ν_0/c [cm^{-1}]	Linewidth $\delta\nu/c$ [cm^{-1}]	Gain factor g_S [10^{12} m/W]	Excitation wavelength [nm]	Ref.
$Ba_2NaNb_5O_{15}$	650		67	694	[72Mai]
Calcite	1086	1.1	1.4	530	[69Col]
$CuAlS_2$	314		21,000	514	[97Bai]
GaP	403		19,000	632	[97Bai]
$^6LiNbO_3$	256		180	694	[72Mai]
$^7LiNbO_3$	256		89	694	[72Mai]
$^6LiTaO_3$	600		43	694	[72Mai]
Quartz	467		0.15	527	[67Wig]

(c) Gases

Medium	Stokes shift ν_0/c [cm^{-1}]	Differential scattering cross section $d\sigma/d\Omega$ [10^{36} m^2 sr^{-1}]	Dephasing time T_2 [ps]	Gain factor g_S [10^{12} m/W]	Excitation wavelength [nm]	Ref.
H_2, Q(1)	4155	1.2	208	9.7	1064	[86Han]
H_2, Q(1)	4155	79	208	27.6	532	[86Han]
D_2, Q(2)	2987	2.0	150	3.7	1064	[86Han]
D_2, Q(2)	2987	8.0	150	10	532	[86Han]
Methane, Q	2917	7.0	16	3.3	1064	[86Han]
Methane, Q	2917	270	16	8.6	532	[86Han]

4.3.3.2 Stimulated Brillouin scattering (SBS) and stimulated thermal Brillouin scattering (STBS)

Stimulated Brillouin scattering was extensively studied in liquids, solids, and gases. In many substances it is the dominant process under stationary conditions and occurs generally in backward direction. The scattering originates from two coupling mechanisms between the electromagnetic field and the medium: electrostriction and absorption. In transparent media only electrostriction is relevant. In absorbing media the second contribution called Stimulated Thermal Brillouin Scattering (STBS) is caused by absorption-induced local temperature changes leading to propagating density waves. The frequency dependencies of the gain factors for the two mechanisms are different. The peak values of stimulated gain are given by:

$$g_B^e = \frac{(\partial\varepsilon/\partial\rho)_T^2\,\omega_S^2\,\rho_o}{2\,c^3\,n_S\,v\,\Gamma_B} \tag{4.3.14}$$

for the electrostrictive contribution (superscript "e"), and by

$$g_B^a = \frac{\alpha\,(\partial\varepsilon/\partial\rho)_T\,\omega_S\,\beta_T}{4\,c\,n_S\,C_p\,\Gamma_B} \tag{4.3.15}$$

for STBS. Here $(\partial\varepsilon/\partial\rho)_T$ is the change of the relative dielectric constant with mass density ρ at constant temperature T. ρ_o is the equilibrium density value. v denotes the sound velocity at

frequency $\omega_o = \omega_L - \omega_S$ (see (4.3.4) for backward scattering, $\theta = 180°$). The parameters in (4.3.15) are the absorption coefficient of the laser intensity α and the relative volume expansion coefficient β_T. The half-width $\Gamma_B = \pi\ \delta\nu$ of the corresponding spontaneous Brillouin line that displays an approximately quadratic frequency dependence also enters the expressions above. For liquids one can write:

$$\frac{\Gamma_B}{\omega_o^2} = \frac{\frac{4}{3}\,\eta_S + \Lambda\left(\frac{1}{C_V} - \frac{1}{C_p}\right) + \eta_V}{2\,\rho_o\,v^2}\ , \tag{4.3.16}$$

where η_S and η_V, respectively, denote the shear and volume viscosity; the latter is to some extent frequency-dependent via relaxation phenomena. Λ is the thermal conductivity. C_V and C_p are the specific heat per unit mass at constant volume and pressure, respectively. The phonon lifetime τ of the involved acoustic phonons with circular frequency ω_o is related to the linewidth by $\tau = T_2/2 = 1/(2\,\Gamma_B)$. The peak gain value g_B^a increases proportional to α and is of same order of magnitude as g_B^e for $\alpha \approx 1\ \mathrm{cm}^{-1}$.

The total frequency-dependent gain factor for the (first-order) Stokes component of SBS including STBS is given by

$$g(\omega_S) = \frac{g_B^e\,\Gamma_B^2}{(\omega_S - \omega_L + \omega_o)^2 + \Gamma_B^2} - \frac{g_B^a\,2\,\Gamma_B\,(\omega_S - \omega_L + \omega_o)}{(\omega_S - \omega_L + \omega_o)^2 + \Gamma_B^2}\ . \tag{4.3.17}$$

The maximum contribution of STBS is red-shifted relative to the Brillouin line and occurs at $\omega_S = \omega_L - \omega_o - \Gamma_B$. In the blue wing of the Brillouin Stokes line the mechanism produces stimulated loss. Equation (4.3.17) states that the Stokes shift observed in the stimulated Brillouin scattering of absorbing media in the generator or oscillator setup – occurring at the peak value of $g(\omega_S)$ – is modified compared to the spontaneous Brillouin line.

A list of frequency shifts observed in SBS of transparent media is presented in Table 4.3.3 where values for the Brillouin linewidth $\delta\nu$ and the gain parameters g_B^a/α and g_B^e are also compiled. The relaxation time T_2 $(= 1/\pi\ \delta\nu)$ in condensed matter is in the order of 10^{-9} s so that SBS is close to steady state for giant laser pulses with $t_p \approx 10^{-8}$ s (if self-focusing is avoided), but is of transient character in the subnanosecond time domain.

4.3.3.3 Stimulated Rayleigh scattering processes, SRLS, STRS, and SRWS

Three mechanisms can be distinguished:

1. Stimulated Rayleigh Line Scattering in transparent substances, SRLS, by electrostrictive coupling to non-propagating density changes,
2. Stimulated Thermal Rayleigh Scattering, STRS, by absorptive coupling similar to the STBS case, and
3. Stimulated Rayleigh Wing Scattering, SRWS, in liquids by orientational changes of anisotropic molecules.

The frequency shifts of the Stokes component of the first two cases are considerably smaller than for SBS. SRLS is difficult to observe because of the small gain factor and the relatively long relaxation time $T_2 \approx 10^{-8}$ s for backward scattering leading to transient scattering for nanosecond pulses.

Table 4.3.3. Stimulated Brillouin scattering in backward direction: frequency shift, linewidth, and gain factor.

Medium	Stokes shift ν_0/c [cm^{-1}]	Linewidth $\delta\nu$ [MHz]	Gain coefficient g_B^a/α (calculated) [cm^2 / MW]	Gain factor g_B^e (calculated) [cm / MW]	Gain factor g_B^e (measured) [cm / MW]	Ref.
Acetic acid	0.152					[67Wig]
Acetone	0.154	180	0.022	0.017	0.020	[70Poh]
Aniline	0.259					[67Wig]
Benzaldehyde	0.224					[67Wig]
Benzene	0.211		0.024	0.024	0.018	[68Den]
Bromobenzene	0.188					[67Wig]
Carbondisulfide	0.194	75	0.213	0.197	0.068	[97Jo]
Carbontetrachloride	0.146	650	0.0134	0.0084	0.006	[68Den, 70Poh]
Chloroform	0.148					[67Wig]
Cyclohexane	0.180			0.007	0.0068	[68Den]
p-Dichlorobenzene	0.184					[67Wig]
Ethanol	0.152		0.010	0.012		[72Mai]
Fluorinert FC 72					0.006	[97Yos]
Fluorinert FC 75					0.005	[97Yos]
Glass BSC-2	0.866					[67Wig]
Glass DF-3	0.638					[67Wig]
Glycerol	0.386					[67Wig]
n-Hexane		220		0.027	0.026	[68Den, 70Poh]
InSb						[95Lim]
Methanol	0.142		0.013	0.013	0.013	[68Den, 70Poh]
Methylodide	0.166					[67Wig]
Nitrobenzene	0.228					[67Wig]
m-Nitrotoluene	0.229					[67Wig]
n-Nitrotoluene	0.217					[67Wig]
Octanol	0.194					[67Wig]
Pyridine	0.226					[67Wig]
Quartz	1.16				0.005	[89Agr]
Sulfurhexafluoride (20 atm)					0.0015	[93Fil, 97Jo]
Tetrabromomethane	0.173					[67Wig]
Toluene	0.193	480		0.013	0.013	[68Den, 70Poh]
Water	0.197		0.0008	0.0066	0.0048	[68Den, 77Rys, 94Yos]
p-Xylene	0.199					[67Wig]

1. and 2. The peak value of the stimulated gain for SRLS is given by:

$$g_{RL}^{e} = \frac{(\partial\varepsilon/\partial\rho)_T^2\, \omega_S\, \rho_o\, (\gamma - 1)}{4\, c^2\, n_S^2\, v^2}\ , \tag{4.3.18}$$

where $\gamma = C_p/C_V$. It is interesting to notice that g_{RL}^{e} does not depend on scattering angle ($\omega_S \cong \omega_L$). A finite optical absorption coefficient α of the medium gives rise to a second contribution with peak value:

$$g_{RL}^{a} = \frac{\alpha\, (\partial\varepsilon/\partial\rho)_T\, \omega_S\, \beta_T}{2\, c\, n_S\, C_p\, \Gamma_{RL}}\ . \tag{4.3.19}$$

Table 4.3.4. Stimulated Rayleigh scattering: gain factors and linewidth values.

Medium	Gain factor $g^{\mathrm{e}}_{\mathrm{RL}}$ [cm/MW]	Gain coefficient $g^{\mathrm{a}}_{\mathrm{RL}}(\mathrm{max.})/\alpha$ [cm^2/MW]	Linewidth $\delta\nu$ [MHz]	Reference
Acetone	2	0.47	21	[70Rot]
Benzene	2.2	0.57	24	[70Rot]
Carbondisulfide	6	0.62	36	[70Rot]
Ethanol		0.38	18	[70Rot]
Methanol	8.4	0.32	20	[70Rot]
Tetrachloromethane	2.6×10^{-4}	0.82	17	[70Rot]
Water	0.02	0.019	27.5	[70Rot]

Here $\Gamma_{\mathrm{RL}} = \pi\,\delta\nu$ is the halfwidth (HWHM) of the spontaneous Rayleigh line in circular frequency units that originates from the damping of entropy changes via thermal conductivity Λ:

$$\Gamma_{\mathrm{RL}} = \frac{4\,k_{\mathrm{L}}^2\,\Lambda\,\sin^2(\theta/2)}{\rho_{\mathrm{o}}\,C_p}\ . \tag{4.3.20}$$

Via Γ_{RL} the gain constant $g^{\mathrm{a}}_{\mathrm{RL}}$ strongly depends on scattering angle. The frequency dependencies of SRLS and STRS have opposite sign, leading to the total gain factor:

$$g(\omega_{\mathrm{S}}) = \frac{(g^{\mathrm{e}}_{\mathrm{B}} - g^{\mathrm{a}}_{\mathrm{B}})\,2\,\Gamma_{\mathrm{RL}}(\omega_{\mathrm{L}} - \omega_{\mathrm{S}})}{(\omega_{\mathrm{L}} - \omega_{\mathrm{S}})^2 + \Gamma^2_{\mathrm{RL}}}\ . \tag{4.3.21}$$

For dominant coupling via electrostriction positive gain occurs on the Stokes side, $\omega_{\mathrm{S}} < \omega_{\mathrm{L}}$. Small absorption values, $\alpha > 10^{-3}$ cm^{-1}, can be sufficient for dominant STRS that produces gain on the anti-Stokes side. For zero frequency shift, $\omega_{\mathrm{S}} = \omega_{\mathrm{L}}$, the gain factor vanishes in the steady state, (4.3.21), but not in the transient case. Stimulated scattering in forward scattering is particularly delicate since $\Gamma_{\mathrm{RL}} \to 0$, (4.3.20), and Stokes–anti-Stokes coupling has to be included. Values for g and $\delta\nu$ are listed in Table 4.3.4.

3. Stimulated Rayleigh wing scattering is connected with the overdamped rotational motion of liquid molecules in combination with an anisotropic polarizability tensor. The latter is also involved in the optical Kerr effect enhancing the nonlinear refractive index of the medium (optical self-focusing, self-phase modulation). The maximum steady-state gain factor for SRWS is given by:

$$g_{\mathrm{RW}} = \frac{16\,\pi^2\,N\,\omega_{\mathrm{S}}\,(\alpha_{\parallel} - \alpha_{\perp})^2}{45\,k_{\mathrm{B}}\,T_{\mathrm{o}}\,c^2\,n_{\mathrm{S}}^2}\ . \tag{4.3.22}$$

The difference of the molecular polarizability parallel and perpendicular to the (assumed) molecular axis of rotational symmetry is denoted by $\alpha_{\parallel} - \alpha_{\perp}$. k_{B} is the Boltzmann constant, T_{o} the sample temperature. The frequency dependence of the gain factor is analogous to the previous cases:

$$g(\omega_{\mathrm{S}}) = \frac{g_{\mathrm{RW}}\,2\,\Gamma_{\mathrm{RW}}\,(\omega_{\mathrm{L}} - \omega_{\mathrm{S}})}{(\omega_{\mathrm{L}} - \omega_{\mathrm{S}})^2 + \Gamma^2_{\mathrm{RW}}}\ . \tag{4.3.23}$$

Maximum gain of SRWS occurs for $\omega_{\mathrm{S}} = \omega_{\mathrm{L}} - \Gamma_{\mathrm{RW}}$. The halfwidth Γ_{RW} of the Rayleigh wing line may be taken from spontaneous scattering observations or from the reorientational time τ_{or}. The latter can be derived from spontaneous Raman spectroscopy, NMR, or time-resolved spectroscopy, e.g. transient optical Kerr effect observations: $\tau_{\mathrm{or}} = T_{2,\mathrm{RW}} = 1/\Gamma_{\mathrm{RW}}$. An estimate of the halfwidth may be computed from shear viscosity and the size of the molecules using the Debye theory:

$$\Gamma_{\mathrm{RW}} = \frac{3\,k_{\mathrm{B}}\,T_{\mathrm{o}}}{8\,\pi\,R\,\eta_{\mathrm{S}}}\ . \tag{4.3.24}$$

Here R denotes an effective mean radius of the molecule. The proportionality $\Gamma_{\mathrm{RW}} \propto \eta_{\mathrm{S}}$ was demonstrated experimentally for numerous examples.

Equations (4.3.6), (4.3.22), and (4.3.23) hold for large scattering angles where Stokes–anti-Stokes coupling can be neglected. Close to forward direction simultaneous anti-Stokes scattering enhances the stimulated Stokes scattering, in contrast to SRS. Including the Stokes–anti-Stokes coupling maximum gain is predicted for an optimum scattering angle

$$\theta_{\mathrm{opt}} = \left(\frac{2\, g_{\mathrm{RW}}\, I_{\mathrm{L}}\, c}{n_{\mathrm{L}}\, \omega_{\mathrm{L}}} \right)^{\frac{1}{2}} . \tag{4.3.25}$$

The corresponding gain factor for stimulated amplification in the scattering direction θ_{opt} without frequency shift, $\omega_{\mathrm{S}} = \omega_{\mathrm{A}} = \omega_{\mathrm{L}}$, amounts to:

$$g_{\mathrm{opt}} = 2\, g_{\mathrm{RW}} , \tag{4.3.26}$$

where g_{RW} is given by (4.3.22). For more general cases the reader is referred to the literature, e.g. [72Mai]. Frequency shift and gain factor numbers are compiled in Table 4.3.5.

Table 4.3.5. Frequency shift and gain factor of stimulated Rayleigh wing scattering.

Medium	Frequency shift $\times\, c^{-1}$ [cm^{-1}]	Gain factor G_{RW} [10^{12} m/W]	Reference
Azoxybenzene	0.036		[68Fol]
Benzene		6	[72Mai]
Benzonitrol	0.198		[68Fol]
Benzoylchloride	0.184		[68Fol]
Benzylidenaniline	0.065		[68Fol]
Bromobenzene		14	[72Mai]
1-Bromonaphthalene	0.076		[68Fol]
Carbondisulfide		30	[72Mai]
Chlorobenzene		10	[72Mai]
Chloronaphthalene	0.100		[68Fol]
1,4-Dimethylnitrobenzene	0.090		[68Fol]
m-Dinitrobenzene	0.116		[68Fol]
2,4-Dinitrotoluene	0.098		[68Fol]
Naphthalene	0.5		[68Fol]
Nitroacetophenone	0.105		[68Fol]
o-Nitroaniline	0.107		[68Fol]
p-Nitroanisol	0.075		[68Fol]
Nitrobenzaldehyde	0.101		[68Fol]
Nitrobenzene	0.111	76	[72Mai]
o-Nitrophenol	0.078		[68Fol]
m-Nitrotoluene	0.097		[68Fol]
o-Nitrotoluene	0.133		[68Fol]
p-Nitrotoluene	0.145		[68Fol]
Styrene	0.4		[68Fol]
Toluene		20	[72Mai]